IEEE Access
Multidisciplinary ⋮ Rapid Review ⋮ Open Access Journal

Received January 4, 2018, accepted February 8, 2018, date of publication February 15, 2018, date of current version March 28, 2018.

*Digital Object Identifier 10.1109/ACCESS.2018.2806370*

# Intelligent Modeling Method for a Combined Radiation-Convection Grain Dryer: A Support Vector Regression Algorithm Based on an Improved Particle Swarm Optimization Algorithm

**AINI DAI[1,2], XIAOGUANG ZHOU[1], HAO DANG[1], MUYI SUN[1], AND ZIDAN WU[1]**
[1]School of Automation, Beijing University of Posts and Telecommunications, Beijing 100876, China
[2]Science and Information College, Qingdao Agricultural University, Qingdao 266109, China

Corresponding authors: Xiaoguang Zhou (zxg@bupt.edu.cn) and Zidan Wu (wuzidan@263.net)

This work was supported in part by the BUPT Excellent Ph.D. Students Foundation under Grant CX2017405, in part by the China National Common Wealth Industrial Special Scientific Research Funds for Grain Industry under Grant 201413006, and in part by the 2015 China Special Fund for Grain-Scientific Research in Public Interest under Grant 201513002.

**ABSTRACT** This paper aims to investigate an intelligent model for a combined infrared radiation-convection (IRC) dryer by using a support vector regression (SVR) algorithm based on an improved particle swarm optimization algorithm (IPSO). The IPSO algorithm was designed to optimize the parameters of the SVR algorithm, which has improved the optimization ability of the IPSO [linear decreasing inertia weight (LDIW)] algorithm and the standard PSO algorithm by introducing a relative fitness deviation (FD) to the LDIW equation and by combining a concept of mutation. Based on the data collected from a practical drying experiment, the best IPSO-SVR (LDIW-FD) model for the IRC dryer was successfully constructed, and the prediction performance comparisons of different modeling methods were also made. The resulting IPSO-SVR (LDIW-FD) model has achieved a remarkable predictive accuracy compared with the other models, demonstrating the effectiveness of the proposed model. In addition, a model of concurrent-counter flow drying was also successfully established by using the same method, depicting the proposed method can be readily used to precisely predict different drying processes. This modeling method can give relatively good predictive output information of the nonlinear system, and it may provide an accurate model for the prediction control of grain drying.

**INDEX TERMS** Grain drying, infrared radiation and convection drying, SVR, particle swarm optimization.

## I. INTRODUCTION

Grain drying is one of the most important postharvest techniques in modern agricultural production because it can decrease grain loss by drying the wet grains to specific safety moisture content (MC) levels for the purpose of preserving food from microbial spoilage [1]. As technology advances to new frontiers, the method to dehydrate food is constantly evolving to produce new hybrid drying systems [2], which combining a novel drying method like infrared radiation drying, or microwave drying with the other drying techniques. In our study, a novel combined infrared radiation (IR) and convection (IRC) dryer is designed to raise the effectiveness of drying, which has many advantages, such as its short drying time, the good quality of the final dried product, and its energy-saving capability, in addition to its lower price compared to microwave and vacuum drying methods and the ability to combine it with other drying techniques [3].

Modeling of the grain drying process is an important approach because it can provide an accurate mathematical model for controlling the grain drying system and can facilitate better understanding of the grain drying mechanism for practical production. However, grain drying is a complicated heat and mass transfer process with the characteristics of long delay, strong nonlinearity, uncontrolled disturbances and coupling of key variables, which increase process uncertainty [4]. Thus, it is not easy to build a precise mathematical model [5], [6]. In this paper, the drying mechanism of IRC smart dryer is a typical nonlinear process in industrial engineering, hence the control of the IRC drying is a challenging task.

The IRC (or IR) drying processes are usually described by some traditional empirical and semi-empirical differential equations in the research literatures and the references therein [7]–[17], which are generally based on some assumptions and observations, and do not consider the many complex influencing factors of drying. These simplifications are assumed to affect the accuracy of control when using these models for control purpose. Although some complex mechanism models have been established, the methods of solving the equation and boundary conditions are complex; which are not suitable for the control of grain drying in practice.

A promising approach is to use artificial intelligence (AI) approaches such as artificial neural network (ANN) or fuzzy logic (FL) to estimate uncertain continuous nonlinear functions, and then to construct controllers by combining nonlinear control algorithms such as adaptive control, backstepping control, sliding mode control and evolutionary algorithms (EA) or their combinations. The many studies on learning systems based control have proved that the ANN and FL of AI technologies are extraordinarily applicable for the nonlinear systems with highly uncertainties (see the literatures [18]–[24] and the references therein). For instance the ANN application in the wind turbine control shown in [18], and in [19] an adaptive fuzzy control method is presented for a class of nonaffine stochastic nonlinear systems via backstepping; in [20] an observer-based fuzzy output feedback control algorithm is proposed by using backstepping and fuzzy systems' universal approximation capability for stochastic nonlinear multiple time-delay systems; in [21] an adaptive intelligent control of nonaffine nonlinear time-delay systems with dynamic uncertainties is investigated; in [22] an intelligent adaptive control algorithm is presented by combining the adaptive backstepping technique with the neural networks' approximation ability; in [23] an adaptive neural control of MIMO nonstrict-feedback nonlinear systems with time delay is designed; in [24] the T–S fuzzy modeling approach is applied to represent the underlying nonlinear system to make the obtained condition easily verified, and etc. The many valuable simulation results of the above methods have demonstrated that FL or ANN systems have excellent approximation ability for the unknown nonlinearities in system dynamics.

Currently, many scholars have already successfully described the drying characteristics of many agricultural products by using ANN [25]–[27], and there are also many researchers who have paid attention to the control of different drying processes by using ANN, or FL algorithms, or the combination of ANN and FL. Such as Wu et al. [28] have proposed an adaptive neuro-fuzzy inference system for a bulk tobacco flue-curing control process; Li et al. [29] have proposed a recurrent self-evolving fuzzy neural network (RSEFNN) predictive control scheme for microwave drying; O. F. Lutfy et al. have designed an intelligent simplified type 2 neuron-fuzzy controller for a belt dryer [1]; in our study works a genetically optimized fuzzy Immune PID controller for the IRC dryer [30] and a double fuzzy immune PID controller [31] were proposed, respectively. In addition, in our study [32], we have also developed a precisely ANN model of back propagation for the IRC drying.

In addition to ANN, support vector machine (SVM) is another representative artificial intelligent algorithm, which has several advantages over ANN, including better generalization ability, easier training, a mechanism for modeling structured data and, most importantly, the generation of a unique solution [33], while ANN faces issues such as becoming trapped in local minima, slow learning and the need to tune meta-parameters [34]. Furthermore, compared to conventional learning methods, which are based on large-scale samples, SVM is very suitable for learning based on small-scale samples [35]. So, SVM will be a suitable method for the application of intelligent control in the grain drying than ANN.

SVM was first developed for solving classification tasks, and then was used to solve regression tasks, in which case it is called Support Vector Regression (SVR). SVR has been widely used in the last decades due to its many advantages [36]–[40]. However, there are currently no studies on the modeling of grain drying with SVR in the literatures. So, in this study, SVR is selected to approximate the nonlinear relationship of IRC drying, and in the results part we have also compared the prediction performance of the SVR model with the ANN model.

In the SVR model, $\gamma$ (the coefficient of the kernel function that is adopted in the SVR model) and C (the penalty factor of the SVR model) are user-determined parameters, which need to be optimized. Jaime Alonso used a procedure called internal grid search to obtain the best parameters with 2-fold cross-validation, which was repeated five times, to predict carcass weight in beef cattle [39], as did Liu *et al.* [40]. Grid search based on cross-validation (CV) for realizing optimal parameter selection in SVM has proved to be effective. With this approach, C and $\gamma$ can be searched first over a wide range and then in a narrow range to obtain more precise values, thereby avoiding over-fitting and enabling the model to obtain more precise prediction results. Heuristic algorithms such as Genetic Algorithm (GA) and the Particle Swarm Optimization (PSO) algorithm are also good choices for finding the best parameters of SVR.

The PSO algorithm was introduced by Kennedy and Eberhart in 1995 [41], which is an optimization technique and belongs to the category of artificial intelligence techniques. As an emerging evolutionary algorithm, it follows a simple principle that is easy to implement. The PSO algorithm is effective in solving many nonlinear optimization problems. Unlike many traditional mathematical methods, this optimization method does not require any gradient information about the objective or error function and can obtain the best solution independently [42]. This method is also less dependent on the starting point in obtaining the globally optimal solution.

Due to its excellent characteristics of simplicity and fast convergence, the PSO algorithm has been widely applied in many domains, such as multi-objective optimization, mode identification, and signal processing [43]–[45]. However, the PSO algorithm has some limitations, such as: premature convergence and failure to obtain the globally optimal results [46]. To improve the performance of the standard PSO algorithm, some investigations have been carried out on combining it with other methods, e.g., by introducing some mechanism into the standard PSO algorithm and modifying the inertial weights [47], [48]. For example, to improve the global searching ability in early iterations and enhance the local optimization ability in later iterations, Shi and Eberhart [49] proposed a LDIW equation in, in addition, to avoid becoming trapped in the local optima, the conception of mutation can be introduced.

Hence, based on the above observations, we investigate a model for the grain drying process, i.e., support vector regression modelling method based an improved particle swarm optimization algorithm. The main contributions of this paper are as follows: 1) SVR algorithm is an attractive solution to deal with the highly nonlinear process of engineering. Compared to the exiting traditional empirical models, it can comprehensively consider more influence factors of grain drying and can be readily used to describe different drying processes regardless of the dryer type; 2) compared to ANN, SVR is based on statistical learning theory, and it is more fit to learn based on small-scale samples. Hence, it will be a better choice to be used in the practical drying control by modeling the complex IRC drying process; 3) A nonlinear optimization algorithm -an improved PSO algorithm (IPSO (FD-LDIW)) is firstly proposed, which introduces a Fitness Deviation (FD) equation into the LDIW equation and combines a concept of mutation. It further improves the optimization ability of the standard PSO algorithm and the IPSO algorithm based on the LDIW equation proposed by the scholar Y. Shi (IPSO(LDIW)).

The rest of this paper are arranged as follows: the material and methods principle are given in Section II. A prediction model for the IRC dryer has been developed by using the IPSO-SVR (LDIW-FD) method to predict the outlet grain MC of the IRC dryer, and the simulation results and comparisons of the prediction performance are also presented in Section III. The results discussion is given in Section IV, which further demonstrate the effectiveness of the SVR modeling method. Finally, the work has been concluded in Section V.

## II. MATERIAL AND METHODS

### A. EXPERIMENTAL SYSTEM

The data that were used in this study were collected from the IRC grain drying system that had been put into use in Harbin Development Zone, Binxi town, China, Dongyu Machinery Co. Ltd. Fresh, mature corn was purchased from a local farm (an agricultural area in northern China). The self-designed IRC grain drying experiment system is mainly composed of the mechanical structure, which is shown in Fig. 1, and

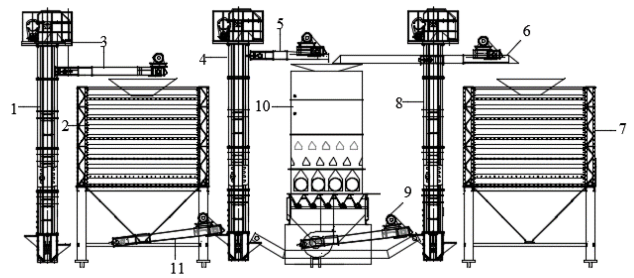


**FIGURE 1.** Mechanic structure diagram of the grain drying system. 1, 4, 8: Bucket elevators; 2: Wet grain bin; 3, 5, 6, 9, 11: Belt conveyor; 7: Dried grain bin; 10: Dryer.

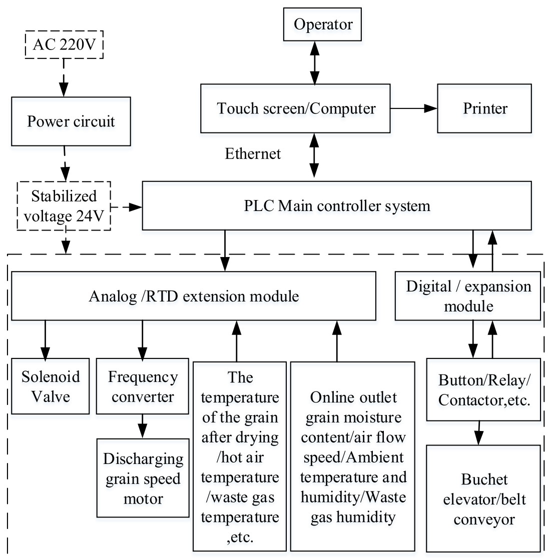


**FIGURE 2.** Control scheme diagram of the grain dryer.

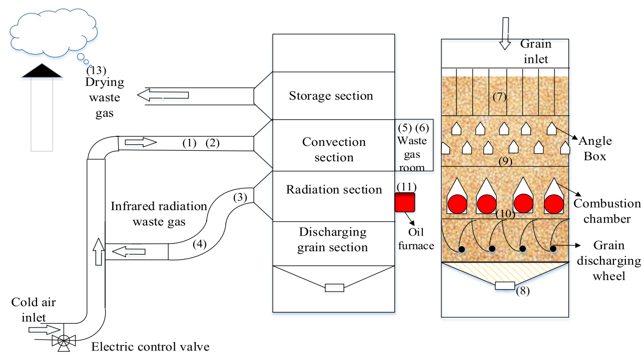


**FIGURE 3.** Schematic diagram of the IRC grain dryer. Sensors: (1) Hot air flow rate, (2) Hot air temperature, (3) Infrared radiation waste gas temperature, (4) Infrared radiation waste gas flow rate, (5) Drying waste gas humidity, (6) Drying waste gas temperature, (7) Inlet grain temperature and moisture, (8) Outlet grain temperature and moisture, (9) Grain temperature after convection drying, (10) Grain temperature after infrared radiation drying, (11) Combustion tube temperature, (12) Flue gas temperature, (13) Ambient temperature and humidity.

the control structure, which is shown in Fig. 2 [30]–[32]. As shown in Fig. 1, the mechanical system consists of the following parts: a wet grain bin, a 5HSHF10-type grain dryer (2.06 m $\times$ 1.30 m $\times$ 5.3 m), a dried grain bin, 3 bucket elevators, and 5 belt conveyor machines. Fig. 3 shows the structure of the designed 5HSHF10-type grain dryer, which is rectangular in shape and consists of four sections: a storage grain section (0.8 m in height), a convection section (1.1 m in height), a radiation section (0.8 m in height), and a discharging grain section (1.2 m in height). The convection section is a combination design and there are three kinds of drying techniques to choose in the convection section: concurrent flow drying, concurrent-counter flow drying, and mixed flow drying. Thus, the dryer combines the advantages of infrared radiation drying technology and convection drying technology: the infrared radiation material on the surface of the radiation tube absorbs the heat that is generated by the oil furnace to carry out radiation drying in the radiation section, while the waste gas that is generated by the infrared radiation drying is used to carry out the convection drying in the convection section by mixing with a suitable amount of cold air in the main hot air channel. The drying process is as follows: the wet grains in the wet grain bin flow into the dryer from the top of the dryer; pass through the storage section, the convection section, the radiation section and the discharging section in sequence; and, finally, are evacuated from the bottom of the discharging grain section according to the set grain flow rate. In a circulating drying mode, if the outlet grain moistures haven't reached the target value, according to the moisture that is detected by the outlet grain moisture sensor, the grains will enter the dryer again through the top entrance by reversing belt conveyor 6; otherwise, the grains that meet the target MC will be discharged into the dried grain bin by advancing belt conveyor 6 and the drying process will end. In this paper, we mainly consider the modeling of the circulating drying process of the IRC dryer using an improved PSO-SVR (LDIW-FD) method.

As shown in Fig. 2, the programmable controller technology (PLC) and the frequency converter are adopted in the control system and 21 temperature values (measurement accuracy: $\pm 0.1 \sim \pm 0.5°C$), 3 hot wind speed values (measurement accuracy: $\pm 0.2\%$ reading $\pm 0.5\%$ full range), 2 humidity values (measurement accuracy: $\pm 3.0\%$ RH within 20%-80% RH) and the outlet and inlet grain MC values (measurement accuracy: within $\pm 0.2\%$ (wb)) can be detected in real time by the sensors that are installed in the IRC dryer. The detected data are collected by the PLC and transmitted to a computer or a touch screen for storage, display and calculation through Ethernet communication, and 3 bucket elevators, 5 grain belt conveyor machines and other devices are controlled in the control center. Throughout the entire grain drying process, the speed control of the discharging grain motor can be adjusted automatically by an intelligent control algorithm at every time interval or adjusted manually by an experienced worker according to the detected drying parameters

In this paper, the data that are used to model the IRC drying were obtained from a drying experiment that was performed on the IRC grain dryer (corn concurrent flow and radiation) on November 25, 2015. During the experiment, the ambient temperature ranged from $-19°C$ to $-9°C$, the ambient

**TABLE 1. Descriptions of the features of the model dataset used in the paper.**

| Name | Abbreviation | Unit | Range | Max | Min |
|---|---|---|---|---|---|
| Size | Size | | 1-274 | 274 | 1 |
| Drying time | $D_t$ | min | 31-304 | 304 | 31 |
| Inlet grain moisture content (wet basis). | $M_{in}$ | % | 13-33 | 32.6 | 13.2 |
| Inlet grain temperature | $T_{in}$ | °C | 24-38 | 38.0 | 25.5 |
| Outlet grain moisture content (wet basis) | $M_{out}$ | % | 12-29 | 29.0 | 12.6 |
| Outlet grain temperature | $T_{out}$ | °C | 33-52 | 51.0 | 33.8 |
| IR grain temperature | $T_{ir}$ | °C | 42-66 | 65.5 | 42.9 |
| Convection grain temperature | $T_{cv}$ | °C | 44-59 | 58.8 | 44.4 |
| Hot air temperature | $T_h$ | °C | 97-124 | 123.2 | 98.5 |
| Discharging grain motor speed | $V$ | Hz | 10-20 | 20 | 10 |

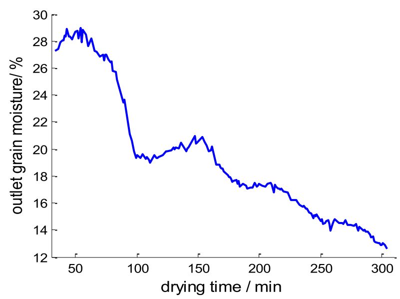


**FIGURE 4. Corn drying curve of the IRC dryer.**

relative humidity ranged from 60% to 70%, the hot air speed was approximately 12 m/s, and the initial average MC of the corn was approximately 28% (wet base). The inlet/outlet grain MC sensors had been validated in advance by a 105°C standard oven moisture measuring method (GB5497-1985). The data were collected every minute when the radiation temperature reached 380°C and the hot air temperature reached 120°C after running the IRC dryer for 0.5 hours.

The collected data were processed by eliminating unreasonable data, such as large random errors that were caused by system failures or obviously inaccurate measurements that were caused by the icing phenomenon inside the grain. A dataset of $274*9$ numerical descriptions of grain drying was finally selected for predicting the outlet grain MC of the IRC dryer, in which each row represents the parameter values for one minute and the 9 columns represent 9 main factors that affect grain drying: the drying time ($D_t$), the inlet grain moisture content ($M_{in}$) and temperature ($T_{in}$), the outlet grain MC ($M_{out}$) and temperature ($T_{out}$), the grain temperature at the infrared radiation section ($T_{ir}$), the grain temperature at the convection section ($T_{cv}$), the hot air temperature at the convection section ($T_h$), and the discharging grain motor speed ($V$). In this paper, the outlet grain MC model for the radiation and concurrent drying of the IRC dryer was designed using an IPSO-SVR (LDIW-FD) algorithm. Table 1 describes the model dataset that is used in the paper, and the drying curve of the dataset is shown in Fig. 4.

### B. SUPPORT VECTOR REGRESSION (SVR)

Support vector machine (SVM) is a machine learning method, which was proposed by Vapnik et al. It is based on statistical learning theory and the structural risk minimization (SRM) principle [39]. The most commonly used type of SVR is $\varepsilon$-SVR, which is briefly introduced in the following [50], [51].

A set of training data is given as $\{(x_i, y_i) \mid x_i \in R^n, y_i \in R^l\}$, $i = 1, \ldots, m$, where $x_i$ is the input and $y_i$ is the target output. The purpose of SVR is to find a function $f(x)$, as shown in (1), that is close to the target value $y_i$.

$$f(x) = w^T \phi(x) + b \tag{1}$$

where $\phi(x)$ is a transformation function that maps each input vector $x$ in the Euclidean space into $X = \phi(x)$ in the high-dimensional feature space; $w \in \mathcal{R}^n$ is a weight vector; the superscript $T$ denotes transpose; and $b \in \mathcal{R}$ is a bias value.

In this study, an $\varepsilon$-SVR model is designed. The $\varepsilon$-SVR method uses a new type of loss function, called the insensitive loss function, which has at most $\varepsilon$ deviation from the obtained targets $y_i$ for all training data [51]. Only when the absolute value of the deviation is greater than a certain value is the loss calculated; this is equivalent to building a zone of width $2\varepsilon$ of the interval by taking $f(x)$ as the center. If the training sample falls into the zone, it is considered correct.

Thus, the SVR primal problem can be formalized as (2):

$$\min \frac{1}{2}\left\|w^2\right\| + C\sum_{i=1}^{m} l_\varepsilon(f(x_i) - y_i) \tag{2}$$

where $C$ is the penalty factor on samples that are outside the $\varepsilon$-error zone and

$$l_\varepsilon(f(x_i) - y_i) = \begin{cases} 0, & \text{if } |f(x_i) - y_i| \le \varepsilon \\ |f(x_i) - y_i| - \varepsilon, & \text{otherwise} \end{cases} \tag{3}$$

Considering the deviation of training samples that are outside the $\varepsilon$-insensitive zone, the slack variables $\xi_i$ and $\xi_i^*$ are introduced, and then the primal problem is rewritten as follows:

$$\min \frac{1}{2}\left\|w^2\right\| + C\sum_{i=1}^{m} (\xi_i + \xi_i^*) \tag{4}$$

$$\text{s.t} \begin{cases} \mathrm{f}(x_i) - y_i \le \varepsilon + \xi_i \\ y_i - \mathrm{f}(x_i) \le \varepsilon + \xi_i^* \\ \xi_i, \xi_i^* \ge 0, \quad i = 1, 2 \ldots\ldots m \end{cases} \tag{5}$$

By introducing a dual set of variables, a Lagrangian function is constructed according to the dual theorem [51], which is shown in (6).

$$\begin{aligned} &\mathrm{L}\left(\mathrm{w}, \mathrm{b}, \xi_i, \xi_i^*, \alpha_i, \alpha_i^*, \mu_i, \mu_i^*\right) \\ &= \frac{1}{2}\|w\|^2 + C\sum_{i=1}^{m} (\xi_i + \xi_i^*) \\ &\quad - \sum_{i=1}^{m} (\mu_i \xi_i + \mu_i^* \xi_i^*) \\ &\quad + \sum_{i=1}^{m} \alpha_i (\mathrm{f}(x_i) - y_i - \varepsilon - \xi_i) \\ &\quad + \sum_{i=1}^{m} \alpha_i^* (y_i - \mathrm{f}(x_i) - \varepsilon - \xi_i^*)) \end{aligned} \tag{6}$$

where $\alpha_i$, $\alpha_i^*$, $\mu_i$, and $\mu_i^*$ are the Lagrangian multipliers.

Let the partial derivatives of $L$ with respect to the primal variables $(w, b, \xi_i, \xi_i^*)$ be zero for optimality:

$$\begin{cases} \dfrac{\partial L}{\partial w} = 0 \rightarrow w = \sum_{i=1}^{m} (\alpha_i - \alpha_i^*)\phi(x_i) \\ \dfrac{\partial L}{\partial b} = 0 \rightarrow \sum_{i=1}^{m} (\alpha_i - \alpha_i^*) = 0 \\ \dfrac{\partial L}{\partial \xi_i} = 0 \rightarrow C = \mu_i + \alpha_i \\ \dfrac{\partial L}{\partial \xi_i^*} = 0 \rightarrow C = \mu_i^* + \alpha_i^* \end{cases} \tag{7}$$

Substituting (7) into (6), we obtain the dual problem of $\varepsilon$-SVR, which is shown in (8):

$$\begin{aligned} \max_{\alpha,\alpha^*} &\sum_{i=1}^{m} y_i (\alpha_i^* - \alpha_i) - \varepsilon(\alpha_i^* + \alpha_i) - \frac{1}{2}\sum_{i=1}^{m}\sum_{j=1}^{m} \\ &\times (\alpha_i^* - \alpha_i)\left(\alpha_j^* - \alpha_j\right) K(x_i, x_j) \end{aligned} \tag{8}$$

$$\text{such that } \sum_{i=1}^{m} (\alpha_i - \alpha_i^*) = 0;\ 0 \le \alpha_i,\ \alpha_i^* \le C \tag{9}$$

where $K(x_i, x_j) = \phi(x_i)^T \phi(x_i)$ is the kernel function.

For a nonlinear system such as grain drying, one of the most widely adopted kernel functions is the radial basis function (RBF), which shown in (10) [39]. It has fewer required parameters and can manage the nonlinear relationship well.

$$K(x, x_j) = \exp(-\gamma \left\|x - x_j\right\|^2) \tag{10}$$

The above process satisfies the Karush–Kuhn–Tucker condition, which is shown in (11):

$$\begin{cases} \alpha_i (\mathrm{f}(x_i) - y_i - \varepsilon - \xi_i) = 0 \\ \alpha_i^* \left(y_i - \mathrm{f}(x_i) - \varepsilon - \xi_i^*\right) = 0 \\ \alpha_i \alpha_i^* = 0,\ \mu_i \mu_i^* = 0 \\ (C - \alpha_i)\xi_i = 0,\ \left(C - \alpha_i^*\right)\xi_i^* = 0 \end{cases} \tag{11}$$

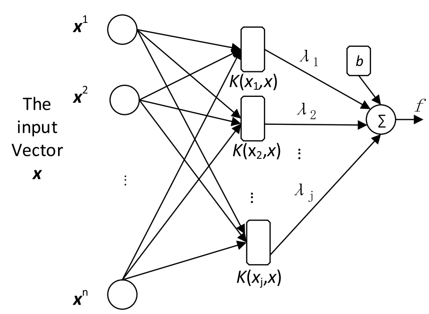


**FIGURE 5.** The model structure of SVR.

By solving (8) (9) using the Sequential Minimal Optimization (SMO) algorithm, which was first proposed by John C. Platt for obtaining the optimal solutions of convex programming problems, the best-estimate function $f(x)$ can be expressed in the form that is shown in (12), and the model structure that is designed in this paper is shown in Fig. 5:

$$f(x) = \sum_{j=1}^{n} (\alpha_j^* - \alpha_j)K(x, x_j) + b = \sum_{j=1}^{n} \lambda_j K(x, x_j) + b \tag{12}$$

where $\lambda_j = \alpha_j^* - \alpha_j (0 \leq \alpha_j, \alpha_j^* \leq C)$, $\lambda_j$ is the weight coefficient of the support vector, $x_j$ is the support vector, and $n$ is the number of support vectors.

The kernel function $K(x, x_j)$ enables operations to be performed in the input space rather than in the potentially high-dimensional feature space. In this way, computation is avoided in the high-dimensional space and the result is equivalent.

### C. IMPROVED PSO ALGORITHM FOR OPTIMIZING THE SVR PARAMETERS

The PSO algorithm is based on research on swarms, such as bird flocking and fish schooling [42]. According to the results on bird flocking, birds search for food by flocking, and the most effective way for each bird to find food is to search the area around the bird that is nearest to the food.

In this paper, we used an improved PSO algorithm (IPSO) to search for the optimal SVR parameters for constructing the best SVR model for predicting the outlet grain MC. The adopted fitness function of the IPSO algorithm is the prediction accuracy, which is based on the cross-validation (CV) method. The idea of the CV method is as follows: The original data are grouped into two sets, namely the training set and the validation set, wherein the training set is used to train the model and the validation set is used to validate the model. Then, the prediction accuracy of performance indicators on the validation set is taken as the prediction accuracy of the model.

To obtain the optimal parameters, the PSO algorithm first arranges $D$ particles at random locations to form the swarm ($X = \{X_1, X_2, X_3, \ldots, X_D\}$), and every particle contains $N$ parameters to be identified in the searching range ($X_i = \{X_{i1}, X_{i2}, \ldots, X_{iN}\}$). The fitness value can be used to evaluate the quality of the identified parameters. Each particle represents a potential solution, according to the following information: the current position, the current velocity and the fitness value. A swarm of particles starts flying within the search space to search for optimal points from their initial positions, and flying direction and distance are determined by the velocity, which can be adjusted dynamically. Every particle can remember its personal best position, which is called Pbest, and share information to obtain the global best position of the swarm, which is called Gbest. The particle moves to a new position by tracking Pbest and Gbest within the search space according to its flying experience, and its position is iteratively updated by using the following equations.

$$V_i^{j+1} = WV_i^j + a_1 r_1 (X_i^{Pbest} - X_i^j) + a_2 r_1 (X_i^{Gbest} - X_i^j) \quad (13)$$
$$X_i^{j+1} = X_i^j + V_i^{j+1} \quad (14)$$

where:
$i = 1, 2, \ldots, D$: the $i$th particle;
$V_i^{j+1}$: the particle velocity at new iteration $(j + 1)$;
$V_i^j$: the particle velocity at current iteration $j$;
$W$: inertial weight;
$a_1$, $a_2$: acceleration coefficients, which are between 0 and 2;
$r_1$, $r_2$: random numbers, which are between 0 and 1;
$X_i^{Pbest}$: personal best position of particle $i$;
$X_i^{Gbest}$: global best position of the swarm;
$X_i^j$: position of particle $i$ at current iteration $j$;
$X_i^{j+1}$: position of particle $i$ at new iteration $(j + 1)$.

According to (13), each particle modifies the position by the following information: the current position, the current velocity and the distances between the current position, Pbest and Gbest.

To improve the standard PSO algorithm, the LDIW equation was proposed by Shi and Eberhart [49] shown in (15). In earlier iterations, $j$ is less than $J$, i.e., $W$ is closer to $W_{max}$, which can improve the global search ability, and in later iterations, $j$ is closer to $J$, i.e., $W$ is closer to $W_{min}$, which can enhance the local optimization ability.

$$W = W_{max} - (W_{max} - W_{min}) \frac{j}{J} \quad (15)$$

where $W_{max}$ and $W_{min}$ are the maximum and minimum inertia coefficients, respectively. $j$ is the current iteration number, and $J$ is the given maximum number of iterations. However, the LDIW method still needs to be improved to enhance the search ability: for example, if some particles obtain the best position in early iterations, it is perhaps necessary to search in a local range carefully, rather than just performing simple global search, and similarly, to not only perform simple local search in later iterations. The fitness value describes the quality of the particle, so it can be used to effectively guide the flying velocity of each particle. In this paper, the relative deviation between the fitness value of the current position and the fitness value of the global best position is introduced into the LDIW equation to further enhance the global cognitive ability of each particle; the resulting equation is called the LDIW-FD equation and is shown in (16). The modified equation can enhance each particle's optimization ability according to the fitness value, in both early and late iterations. If the relative deviation of the fitness value is large, the particle's search step can be increased and the optima can be found in a wider searching range; if the fitness value is close to the global best fitness value, the search step can be decreased to search in a local range. Thus, the searching ability will be further enhanced.

$$W = (W_{max} - (W_{max} - W_{min}) \frac{j}{J}) * \frac{fitness\,(j) - global\_fitness}{fitness(j)} \quad (16)$$

where $fitness$ $(j)$ is the particle's fitness value at current iteration $j$ and $global\_fitness$ is the global best fitness value of the swarm.

In addition, the concept of mutation is introduced into the design of the IPSO algorithm to avoid becoming trapped in the local optima: some particles are reinitialized according to a certain probability, which can make some particles jump out of the previous optimal location and search a wider space.

### D. MODEL PERFORMANCE COMPARISON CRITERIA

In this study, we use *MSE* and *R* to evaluate the prediction performance of the designed drying model, which are shown in (17)-(18), as shown at the bottom of this page, where $m$ is the total size of the dataset, $y_i$ is the actual value, and $\hat{y}_i$ is the predicted value. The closer *MSE* is to zero, the better the prediction performance of the model, and the closer $R$ (which ranges from 0 to 1) is to 1, the better the model fits.

## III. MODEL DEVELOPMENT AND SIMULATION RESULTS

### A. MODEL BUILDING

For modeling the IRC dryer, the implementation libsvm is used [52]. The purpose of establishing the model is to predict the drying performance, i.e., the outlet grain MC, as a function of the drying time. Suppose the drying performance at the next time point depends on 9 factors of the current sample time. The outlet grain MC of the next time point can be predicted by the 9 factors of current sample time. The data in Table 1 are randomly divided into two parts: a training dataset of 175∗9 randomly selected items from the entire dataset and a test dataset of 99∗9 items to validate the prediction accuracy of model.

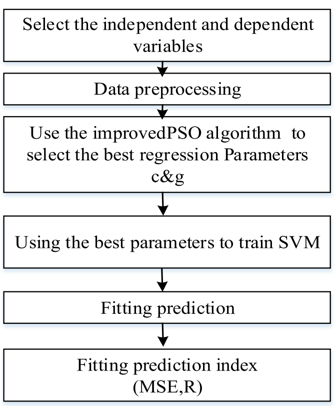


**FIGURE 6.** Flow diagram of model building for the IRC dryer.

We use columns 1-9 of the training dataset as the independent variables and the outlet grain MC of the next sample interval in the dataset as the dependent variable. The flow diagram of model building is shown in Fig. 6.

### B. MODEL REALIZATION

Before training the model, the data should be normalized. The normalization formula is shown in (19):

$$X' = \frac{\left(X'_{\max} - X'_{\min}\right) \times (X_i - X_{\min})}{X_{\max} - X_{\min}} + X'_{\min} \tag{19}$$

where $X_i$, $X_{\max}$, and $X_{\min}$ respectively represent the measured values, the maximum value and the minimum value of the input or output vector in the sample data; $X'_{\max}$ and $X'_{\min}$ respectively represent the maximum and minimum values of the mapping parameter range [1 2]. In the program, we can use the mapminmax function to satisfy the data format requirements.

In this research, 5-fold CV was used, in which the training data were divided into 5 groups, where each group was a subset of the validation set and 4 groups were the training sets. Thus, 5 models were established. In the training, each model was trained with the same values of C and $\gamma$. Finally, the average verification accuracy of the 5 models was taken as the performance index of the IPSO-SVR (LDIW-FD) model, i.e., the fitness function of the IPSO algorithm. The IPSO algorithm searched for the optimal values of $C$ and $\gamma$ in every iteration until the termination condition was satisfied, and then the $C$ and $\gamma$ values with the optimal verification accuracy were used to train the SVR model.

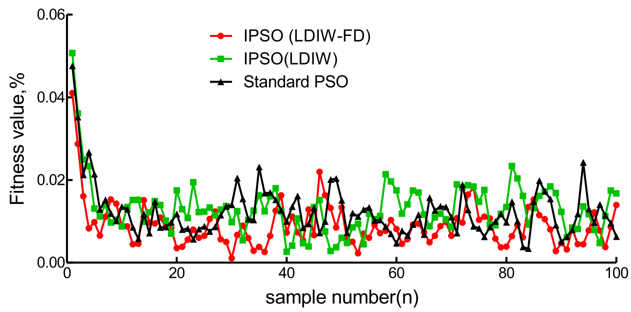


**FIGURE 7.** Fitness curves of different PSO algorithms.

In this paper, to compare the optimization abilities of the PSO algorithms, the IPSO (LDIW-FD), the IPSO (LDIW) and the standard PSO algorithms were used to optimize the SVR model parameters. Each PSO algorithm was run 5 times and the parameters with the minimum fitness value were selected. The initial parameters were as follows: the maximum number of generations: 100; the size of the population: 20; the range of $C$: [0.01,100]; the range of $\gamma$: [0.001,1000]; the mutation probability: 0.9; $W_{max} = 0.9$; $W_{min} = 0.3$; $a_1 = 2$; and $a_2 = 2$. The optimal fitness curves, which were obtained with different PSO algorithms, are shown in Fig. 7,

$$MSE = \frac{1}{m}\sum_{i=1}^{m}\left(y_i - \hat{y}_i\right)^2 \tag{17}$$

$$R = \sqrt{\frac{\left(m\sum_{i=1}^{m}\hat{y}_i y_i - \sum_{i=1}^{m}\hat{y}_i\sum_{i=1}^{m}y_i\right)^2}{\left(m\sum_{i=1}^{m}\hat{y}_i^{\,2} - \left(\sum_{i=1}^{m}\hat{y}_i\right)^2\right)\left(m\sum_{i=1}^{m}y_i^2 - \left(\sum_{i=1}^{m}y_i\right)^2\right)}} \in [0\ 1] \tag{18}$$

**TABLE 2.** Optimized parameters of the SVR model by different PSO algorithms.

| PSO algorithm | $C$ | $\gamma$ | Global fitness value |
|---|---|---|---|
| IPSO (LDIW-FD) | 2.34 | 1.18 | 0.027% |
| IPSO (LDIW) | 41.36 | 0.01 | 0.036% |
| Standard PSO | 77.74 | 0.01 | 0.037% |

**TABLE 3.** 91 support vectors of the PSO-SVR (LDIW-FD) model.

| $x_j$ | (Support vector matrix: j*9) | | | | | | | | | $\lambda_j$ (coefficients of support vector) |
|---|---|---|---|---|---|---|---|---|---|---|
| j | 1 | 2 | 3 | 4 | 5 | 6 | 7 | 8 | 9 | $\lambda_j$ |
| 1 | 1 | 1.9788 | 1.2565 | 1.0157 | 1.0562 | 1.0669 | 1.9078 | 1.125 | 1.9095 | -2.344 |
| 2 | 1.0037 | 2 | 1.224 | 1.0204 | 1.0509 | 1.0565 | 1.879 | 1.0833 | 1.8462 | 1.026 |
| 3 | 1.011 | 1.9448 | 1.3498 | 1.0169 | 1.042 | 1.0381 | 1.8575 | 1 | 1.8748 | 1.928 |
| 4 | 1.0221 | 1.8436 | 1.2492 | 1 | 1.0285 | 1.0156 | 1.8932 | 1.0833 | 1.9318 | -0.872 |
| 5 | 1.0331 | 1.5854 | 1.1599 | 1.007 | 1.0145 | 1.0025 | 1.9229 | 1.0833 | 1.9417 | 1.582 |
| 6 | 1.0515 | 1.5725 | 1.0219 | 1.0221 | 1 | 1.0036 | 1.9671 | 1.4167 | 1.9578 | 2.344 |
| 7 | 1.0588 | 1.4445 | 1 | 1.0163 | 1.0025 | 1.0088 | 1.9821 | 1.4583 | 1.9442 | -2.344 |
| … | … | … | … | … | … | … | … | … | … | … |
| … | … | … | … | … | … | … | … | … | … | … |
| 86 | 1.9154 | 1.0387 | 1.8904 | 1.8813 | 1.8737 | 1.7474 | 1.2554 | 1.4583 | 1.0812 | -2.344 |
| 87 | 1.9338 | 1.0459 | 1.9213 | 1.9121 | 1.8931 | 1.8165 | 1.2164 | 1.4583 | 1.0688 | 1.026 |
| 88 | 1.9449 | 1.0372 | 1.931 | 1.9109 | 1.9082 | 1.8705 | 1.3143 | 1.3333 | 1.062 | 1.928 |
| 89 | 1.9559 | 1.0201 | 1.9383 | 1.9325 | 1.9246 | 1.895 | 1.3041 | 1.4583 | 1.0384 | -0.872 |
| 90 | 1.9632 | 1.0191 | 1.9505 | 1.9761 | 1.9371 | 1.9214 | 1.298 | 1.4167 | 1.0397 | 1.582 |
| 91 | 2 | 1.0046 | 2 | 1.9977 | 2 | 2 | 1.1937 | 1.375 | 1.0012 | 2.344 |

**TABLE 4.** Description of the IPSO-SVR (LDIW-FD) model.

| | SVR parameter selection | | | Model parameters | | | | | Model prediction performance | | | |
|---|---|---|---|---|---|---|---|---|---|---|---|---|
| | | | | | | | | | Training dataset | | Testing dataset | |
| IPSO-SVR (LDIW-FD) | *Best C* | *Best γ* | *ε of SVR* | *K(x,x_j)* | *n* | *b* | $\lambda_j$ | $x_j$ | *MSE* | *R* | *MSE* | *R* |
| | 2.34 | 1.18 | 0.03 | RBF | 91 | -1.51 | 91*1 | 91*9 | $1.69*10^{-4}$ | 99.8% | $2.99*10^{-4}$ | 99.7% |

and the optimal parameter values under different optimization algorithms are shown in Table 2.

The best $C$ and $\gamma$ values that are obtained by IPSO (LDIW-FD) are used to train the SVR model, and the obtained regress model is shown in (20), where $b$ is equal to $-1.51$ and $n$ is equal to 91.

$$f(x) = \sum_{j=1}^{91} \lambda_j K\left(x, x_j\right) - 1.51 \tag{20}$$

Table 3 shows some of the support vectors and the corresponding coefficients of the IPSO-SVR (LDIW-FD) model. The model parameters and the final regress prediction performance values on the training dataset and the testing dataset are described in Table 4. The relative prediction error between the original data and the predicted data are respectively shown in Fig. 8.

### C. MODEL EVALUATION

To evaluate the prediction performances of the IPSO-SVR (LDIW-FD) model; the IPSO-SVR (LDIW) model; the standard PSO-SVR model; the SVR model by the grid search method, which is called GS-SVR; the SVR model by the genetic algorithm, which is called GA-SVR; and the ANN model of back propagation, which is called ANN-BP, were established to predict the outlet grain MC for the IRC dryer. The ANN-BP model consisted of 8 input variables, a hidden layer with 10 initial neurons, 1 output variable, and a learning rate of 0.1, and was trained by the Levenberg-Marquardt (LM) algorithm [32]. The initial parameters of the GA-SVR model were as follows: the maximum number of generations: 100; the size of the population: 20; the range of C: [0.01,100]; the range of $\gamma$: [0.001,1000]; the selection probability: 0.9; and the mutation probability: 0.7.

For effective comparison, each model was trained 5 times. The performance indicators of *MSE* and *R* on the testing dataset are compared in Table 5. The relative error comparisons of the three PSO-SVR algorithms on a sample of 50 testing data are shown in Fig. 9 (a), and the relative error comparisons on a sample of 50 testing data between the IPSO-SVR (LDIW-FD) algorithm and the other AI algorithms are shown in Fig. 9(b).

## IV. RESULTS DISCUSSION

According to the simulation results, the designed IPSO-SVR (LDIW-FD) model has achieved a better prediction accuracy and showed a superior modelling ability for the learning and modelling of nonlinear grain drying processes, which are discussed as follows:

(1) The optimization results comparison of the PSO algorithms: The value of the fitness function and the parameter C can evaluate the optimization ability of the PSO algorithms:

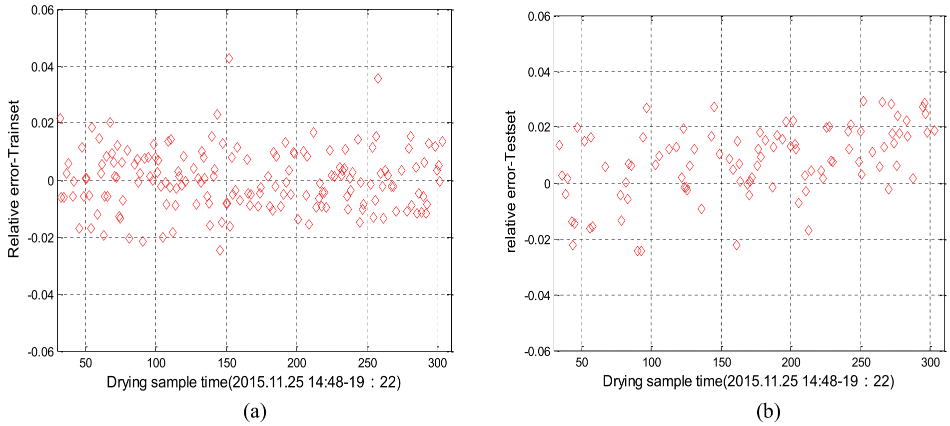


**FIGURE 8.** Relative prediction error of the IPSO-SVR (LDIW-FD) model. (a) Relative prediction error of MC on the training dataset. (b) Relative prediction error of MC on the testing dataset.

**TABLE 5.** Comparison of prediction performances of models on the testing dataset.

| Model | *Best MSE* | *Best R* | *Average MSE* | *Average R* |
|---|---|---|---|---|
| IPSO-SVR (LDIW-FD) | 0.000299 | 99.7% | 0.000353 | 99.6% |
| IPSO-SVR (LDIW) | 0.000346 | 99.6% | 0.000465 | 99.5% |
| PSO-SVR (Standard) | 0.000394 | 99.6% | 0.000473 | 99.5% |
| GA-SVR | 0.000365 | 99.6% | 0.000435 | 99.6% |
| GS-SVR | 0.000434 | 99.6% | 0.000505 | 99.6% |
| ANN-BP | 0.000538 | 99.8% | 0.000775 | 99.8% |

the smaller the value of the fitness function is, the better is the optimization ability of the PSO algorithm. In addition, a smaller value of parameter C would be better because larger C is easy to lead to overfitting of SVR algorithms. As shown in Fig. 7 and Table 2, compared to the other PSO algorithms, the IPSO (LDIW-FD) algorithm has obtained the least fitness function value and the least C value, showing an excellent optimization ability. The global fitness value obtained by the IPSO (LDIW-FD) algorithm is equal to 0.027%, which is about 25% decrease and about 27% decrease than the optimized results of the IPSO (LDIW) and the Standard PSO algorithms, respectively. The SVR parameter C searched by the IPSO (LDIW-FD) is equal to 2.34 that is obviously less than the values searched by the other two PSO algorithms (the C values searched by the IPSO-SVR (LDIW) and by the standard PSO algorithm are, respectively, equal to 41.36 and 77.74). In all, the optimization ability of the IPSO (LDIW-FD) algorithm is obviously superior to the standard PSO algorithm and also has improved the optimization ability of the IPSO (LDIW) algorithm by introducing a relative fitness deviation to the LDIW equation.

(2) The prediction performance of the IPSO-SVR (LDIW-FD) model: As seen from the model prediction results shown in Table 4, the proposed model can precisely predict the outlet grain MC of next sample interval of the IRC dryer, of which the performance indicators *MSE* and *R* computed on the training dataset are, respectively, equal to 0.000169 and 99.8%, and on the testing dataset are, respectively, equal to 0.000299 and 99.7%. From Fig. 8, it can be seen that the relative prediction errors on the training dataset and testing dataset are mostly within ±0.02, which depict the predicted values well fit the actual values and the proposed model can successfully predict the change trends of the outlet grain MC with the drying time.

(3) The prediction performances comparison: As shown in Table 5, all AI algorithms have good prediction performances, of which the *MSE* values are within $10^{-4}$ order of magnitude, depicting AI methods are excellent tools for the learning and modelling of nonlinear processes. Furthermore, as seen from Table 5, the average *MSE* values of the 5 SVR algorithms are all smaller than that of the ANN-BP algorithm, which indicates that the SVR method is superior to ANN-BP algorithm, and SVR method is a better choice for modeling the grain drying process than ANN-BP algorithm.

In addition, as seen in Table 5, compared to the other algorithms, it can be seen that the IPSO-SVR (LDIW-FD) model outperforms the other compared algorithms, and its average *MSE* value is equal to 0.000353, which is the lowest among all the ANN algorithms. Furthermore, the prediction performance of the IPSO-SVR (LDIW-FD) algorithm is obviously improved than the IPSO-SVR (LDIW) algorithm (the average *MSE* of the IPSO-SVR (LDIW) algorithm is 0.000465, which is only slightly less than that of the standard PSO algorithm), and it also has the advantage of avoiding becoming trapped in the local optima.

In addition, as seen from Figure 9 (a) (b), the average relative prediction error of the IPSO-SVR (LDIW-FD) model is the least among all the compared algorithms,

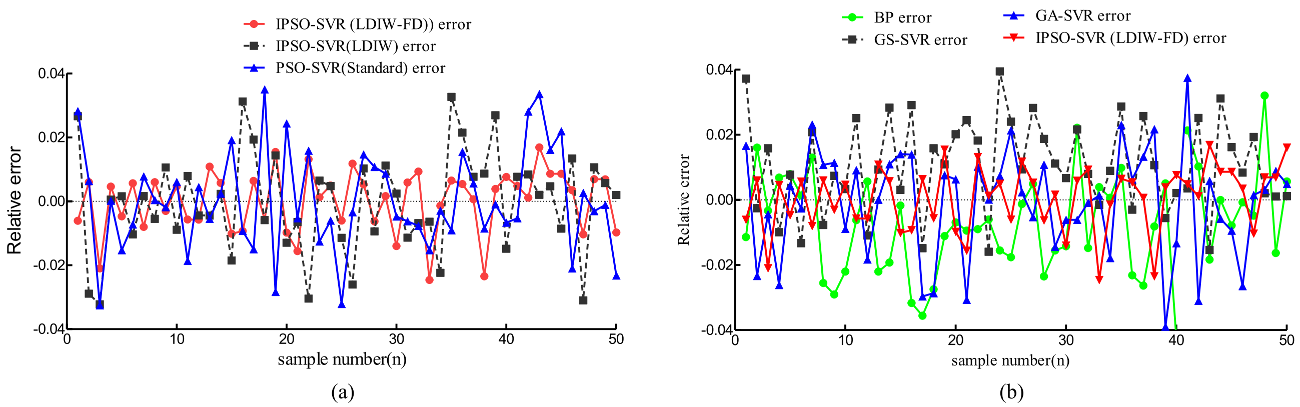


**FIGURE 9. Relative prediction error comparison. (a) Errors comparison among PSO-SVR algorithms. (b) Errors comparison among different AI algorithms.**

which further demonstrates the effectiveness of the proposed algorithm.

(4) Analysis of the predicted kinetic drying curves: Fig. 10 shows that IPSO-SVR (LDIW-FD) model can precisely predict the changes in the outlet grain MC with the drying time under a specific drying-air temperature. At the beginning of drying, the moisture absorption phenomenon within the grain occurred and the closer the grain was to the upper layer, the more obvious was the moisture absorption phenomena, so the outlet grain moisture curves of the IRC dryer at the beginning showed an ascending tendency. After approximately 90 minutes, the grain MC began to decease as the drying time increased. It decreased by 7%-8%, which indicates that a drying cycle was completed. Between 90-180 minutes, the same change trend repeated, but the average drying rate decreased and the grain MC decreased by 3%-4%. After two more cycles of the same change trends, the grain drying process ended. It is inferred that a drying cycle of the IRC dryer is approximately 90 minutes, and 4 cycles of drying are needed to dry to the target value in this circulating drying experiment.

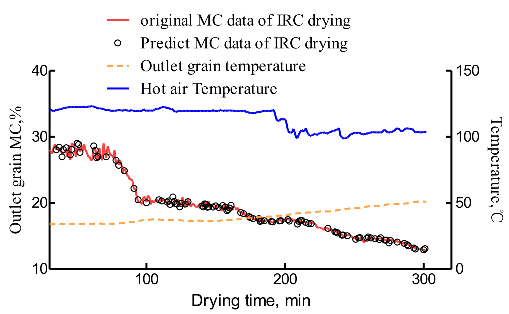


**FIGURE 10. Prediction results analysis under a certain drying condition.**

As shown in Fig. 10, in the first 90 minutes, the grain temperature was basically unchanged when the hot air temperature was maintained at approximately 120°C and the average drying rate was increased; in that period, the water vapor pressure inside the grain was greater than that of the grain surface, and the amount of heat that was absorbed by the grain was roughly balanced with the heat that was utilized for water evaporation, so there was little effect on the grain temperature. During the period from 90-180 minutes, the drying rate decreased and the temperature of the grain increased slightly compared to the first cycle. After 180 minutes, although the temperature of the hot air dropped to 100°C, the grain temperature increased significantly, which indicates that the grain drying process entered a descending stage and the heat for water evaporation decreased.

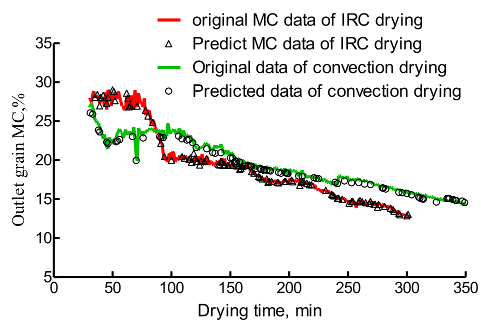


**FIGURE 11. Prediction results comparison of two types of drying processes.**

(5) Prediction ability of different drying techniques: Following the proposed method, a prediction model for the outlet grain MC for concurrent-counter grain drying (which is a type of convection drying technology) was also successfully established using data that were collected from drying experiment on November 28, 2015. This demonstrates that the SVR modeling method can be used to predict the performances of different drying techniques. According to the prediction performance curves of two types of drying processes that shown in Fig. 11, the combined IRC drying method has achieved a faster drying rate, which requires less time to dry to the target grain MC than the convection drying method.

## V. CONCLUSIONS

IRC drying is a complex heat and mass transfer process with the characteristics of long time delay, highly nonlinearity, parameter uncertainties or variations, and etc. It is difficult to build an accurate mathematical model for its kinetic drying process, which substantially increase complexity of control strategies. Facing the problem, ANN and SVR of AI methods are both super tools to model the complex nonlinear system and have a lot of successful applications. Compared to the ANN method, SVR has more advantages, such as: suitable for learning based on small-scale samples, easier training, the generation of a unique solution, and not trapping local minima, so it is more suitable to be used in the modelling of the grain drying than the ANN method.

In this study, taking into account the modelling superiority of the SVR method, we present a SVR model based on an improved PSO optimization algorithm for the IRC dryer, which is called IPSO-SVR(LDIW-FD) for short. The adopted improved PSO algorithm in this model is used to optimize the parameters of the SVR algorithm. The proposed model is developed and simulated by programming in Matlab, and two comparative studies have also been made, one of which is to compare the optimization ability of the IPSO(LDIW-FD) algorithm with the other two PSO algorithms, and the other is to evaluate the prediction performances of different methods of AI

By the comparison results shown in Fig.7 and Table 2, it can be seen that the optimization ability of the IPSO (LDIW-FD) algorithm has been improved compared to that of the IPSO (LDIW) and the standard PSO algorithm, and the global cognitive ability of each particle in the IPSO (LDIW-FD) algorithm is further enhanced by introducing a LDIW-FD equation to the standard PSO algorithm and it avoids becoming trapped in the local optima by combining the concept of mutation. The prediction results of Table 4 and Fig. 8 have shown that the IPSO-SVR (LDIW-FD) model can precisely predict the outlet grain MC of the next sample time on the training dataset and the testing dataset. By the comparison results in Fig. 9 and Table 5, it shows that IPSO-SVR (LDIW-FD) outperforms the other compared AI algorithms, moreover, all SVR models outperform the ANN-BP model in the prediction precision of *MSE*. Therefore, SVR algorithm is a more effective method in modeling the complex grain drying system than ANN-BP. Finally, based on the IPSO-SVR (LDIW-FD) prediction model, the drying performance was analyzed, and a model for concurrent-counter grain drying was also successfully established, which again proves the effectiveness of the SVR modeling method, depicting that it can describe a range of drying experiments while the empirical models are generally only limited to a specific drying experiment.

In all, these above results demonstrate the efficiency of the proposed IPSO-SVR (LDIW-FD) model. Of course, this study has shown that ANN and the other compared models are also fit to a drying system, but the IPSO-SVR (LDIW-FD) model can describe the dying performance more precisely. Furthermore, the IPSO-SVR (LDIW-FD) model can comprehensively consider more influence factors of grain drying and can be readily used to describe any drying processes regardless of the dryer type compared with the traditional empirical and semi-empirical models. In the future study the proposed IPSO-SVR (LDIW-FD) model may provide an accurate model for the intelligent prediction control of the IRC grain drying.

## ACKNOWLEDGEMENTS

The authors of this paper are thankful for the cooperation of the research group, the experimental help of the engineers at Dongyu Machinery Co. Ltd., China, the kindly work of the respected reviewers and editors on the paper.

## REFERENCES

[1] O. F. Lutfy, H. Selamat, and S. B. M. Noor, "Intelligent modeling and control of a conveyor belt grain dryer using a simplified type 2 neuro-fuzzy controller," *Drying Technol.*, vol. 33, no. 10, pp. 1210–1222, 2015.

[2] K. J. Chua and S. K. Chou, "New hybrid drying technologies," in *Emerging Technologies for Food Processing*, D.-W. Sun, Ed. Cambridge, MA, USA: Elsevier, 2005, pp. 535–551.

[3] M. H. Riadh, S. A. B. Ahmad, M. H. Marhaban, and A. C. Soh, "Infrared heating in food drying: An overview," *Drying Technol.*, vol. 33, no. 3, pp. 322–335, 2015.

[4] M. Aghbashlo, S. Hosseinpour, and A. S. Mujumdar, "Application of artificial neural networks (ANNs) in drying technology: A comprehensive review," *Drying Technol.*, vol. 33, no. 12, pp. 1397–1462, 2015.

[5] A. S. Mujumdar, *Handbook of Industrial Drying, Revised and Expanded*, 2nd ed. New York, NY, USA: Marcel Dekker, 1995, pp. 417–424.

[6] Q. Liu and F. W. Bakker-Arkema, "A model-predictive controller for grain drying," *J. Food Eng.*, vol. 49, no. 4, pp. 321–326, 2001.

[7] I. Das, S. K. Das, and S. Bal, "Drying performance of a batch type vibration aided infrared dryer," *J. Food Eng.*, vol. 64, no. 1, pp. 129–133, 2004.

[8] J. Wang, "A single-layer model for far-infrared radiation drying of onion slices," *Drying Technol.*, vol. 20, no. 10, pp. 1941–1953, 2002.

[9] Z. Wu *et al.*, "Drying characteristics of graininess agar under infrared ray and its kinetics model," *Adv. Mater. Res.*, vol. 663, pp. 291–296, Feb. 2014.

[10] X. Lin and X. Wang, "Modeling and evaluation of infrared radiation drying for apple slices," *Trans. Chin. Soc. Agricult. Mach.*, vol. 41, no. 6, pp. 128–132, 2010.

[11] W. Xiangyou, Z. Haipeng, S. Chuanzhu, and Z. Lili, "Infrared radiation drying characteristics and mathematical model for carrot slices," *Trans. Chin. Soc. Agricult. Mach.*, vol. 44, no. 33, pp. 198–202, 2016.

[12] M. R. Islam, K. S. Thaker, and A. S. Mujumdar , "A diffusion model for a drum dryer subjected to conduction, convection, and radiant heat input," *Drying Technol.*, vol. 25, no. 6, pp. 1033–1043, 2007.

[13] R. Ranjan, J. Irudayaraj, and S. Jun, "Simulation of infrared drying process," *Drying Technol.*, vol. 20, no. 2, pp. 363–379, 2002.

[14] T. M. Afzal and T. Abe, "Some fundamental attributes of far infrared radiation drying of potato," *Drying Technol.*, vol. 17, nos. 1–2, pp. 138–155, 1999.

[15] M. J. Lampinen, K. T. Ojala, and E. Koski, "Modeling and measurements of infrared dryers for coated paper," *Drying Technol.*, vol. 9, no. 4, pp. 973–1017, 1991.

[16] R. Dhib, "Infrared drying: From process modeling to advanced process control," *Drying Technol.*, vol. 25, no. 1, pp. 97–105, 2007.

[17] C. Likitrattanaporn and A. Noomhorm, "Effects of simultaneous parboiling and drying by infrared radiation heating on parboiled rice quality," *Drying Technol.*, vol. 29, no. 9, pp. 1066–1075, 2011.

[18] W. Meng, Q. Yang, J. Si, and Y. Sun, "Adaptive neural control of a class of output-constrained nonaffine systems," *IEEE Trans. Cybern.*, vol. 46, no. 1, pp. 85–95, Jan. 2016.

[19] H. Wang, X. Liu, and K. Liu, "Adaptive fuzzy tracking control for a class of pure-feedback stochastic nonlinear systems with non-lower triangular structure," *Fuzzy. Sets Syst.*, vol. 302, pp. 101–120, Nov. 2016.

[20] H. Wang, P. X. Liu, and P. Shi, "Observer-based fuzzy adaptive output-feedback control of stochastic nonlinear multiple time-delay systems," *IEEE Trans. Cybern.*, vol. 47, no. 9, pp. 2568–2578, Sep. 2017.

[21] H. Wang, W. Sun, and P. X. Liu, "Adaptive intelligent control of nonaffine nonlinear time-delay systems with dynamic uncertainties," *IEEE Trans. Syst., Man, Cybern., Syst.*, vol. 47, no. 7, pp. 1474–1485, Jul. 2017.

[22] X. D. Zhao, P. Shi, X. L. Zheng, and J. H. Zhang, "Intelligent tracking control for a class of uncertain high-order nonlinear systems," *IEEE Trans. Neural Netw. Learn. Syst.*, vol. 27, no. 9, pp. 1976–1982, Sep. 2016.
[23] X. Zhao, H. Yang, H. R. Karimi, and Y. Zhu, "Adaptive neural control of MIMO nonstrict-feedback nonlinear systems with time delay," *IEEE Trans. Cybern.*, vol. 46, no. 6, pp. 1337–1349, Jun. 2016.
[24] X. Zhao, Y. Yin, B. Niu, and X. Zheng, "Stabilization for a class of switched nonlinear systems with novel average dwell time switching by T–S fuzzy modeling," *IEEE. Trans. Cybern.*, vol. 46, no. 8, pp. 1952–1957, Aug. 2016.
[25] I. Farkas, P. Reményi, and A. Biró, "Modelling aspects of grain drying with a neural network," *Comput. Electron. Agricult.*, vol. 29, nos. 1–2, pp. 99–113, 2000.
[26] K. Movagharnejad and M. Nikzad, "Modeling of tomato drying using artificial neural network," *Comput. Electron. Agricult.*, vol. 59, nos. 1–2, pp. 78–85, 2007.
[27] G. Çakmak and C. Yıldız, "The prediction of seedy grape drying rate using a neural network method," *Comput. Electron. Agricult.*, vol. 75, no. 1, pp. 132–138, 2011.
[28] J. Wu, S. X. Yang, and F. Tian, "An adaptive neuro-fuzzy approach to bulk tobacco flue-curing control process," *Drying Technol.*, vol. 35, no. 4, pp. 465–477, 2017.
[29] J. Li, Q. Xiong, K. Wang, X. Shi, and S. Liang, "A recurrent self-evolving fuzzy neural network predictive control for microwave drying process," *Drying Technol.*, vol. 34, no. 12, pp. 1434–1444, 2016.
[30] A. Dai, X. Zhou, and X. Liu, "Design and simulation of a genetically optimized fuzzy immune PID controller for a novel grain dryer," *IEEE Access*, vol. 5, pp. 14981–14990, 2017.
[31] A. Dai, X. Zhou, and X. Liu, "A GODFIP control algorithm for an IRC grain dryer," *Math. Problems Eng.*, vol. 2017, 2017, Art. no. 1406292.
[32] A. Dai, X. Zhou, X. Liu, and C. Zhang, "Model of drying process for combined side-heat infrared radiation and convection grain dryer based on bp neural network," *Trans. Chin. Soc. Agricult. Mach.*, vol. 48, no. 3, pp. 351–360, 2017.
[33] E. Colman, W. Waegeman, B. De Baets, and V. Fievez, "Prediction of subacute ruminal acidosis based on milk fatty acids," *Comput. Electron. Agricult.*, vol. 111, pp. 179–185, Feb. 2015.
[34] A. P. Patil and P. C. Deka, "An extreme learning machine approach for modeling evapotranspiration using extrinsic inputs," *Comput. Electron. Agricult.*, vol. 121, pp. 385–392, Feb. 2016.
[35] X.-R. Hou and Z.-J. Zou, "Parameter identification of nonlinear roll motion equation for floating structures in irregular waves," *Appl. Ocean Res.*, vol. 55, pp. 66–75, Feb. 2016.
[36] E. Ghasemi, H. Kalhori, and R. Bagherpour, "A new hybrid ANFIS–PSO model for prediction of peak particle velocity due to bench blasting," *Eng. Comput.*, vol. 32, no. 4, pp. 607–614 , 2016.
[37] P. Tan, C. Zhang, J. Xia, Q.-Y. Fang, and G. Chen, "Estimation of higher heating value of coal based on proximate analysis using support vector regression," *Fuel Process. Technol.*, vol. 138, pp. 298–304, Oct. 2015.
[38] T. Rajaee and A. Boroumand, "Forecasting of chlorophyll—A concentrations in South San Francisco Bay using five different models," *Appl. Ocean Res.*, vol. 53, pp. 208–217, Oct. 2015.
[39] J. Alonso and A. Bahamonde, "Support Vector Regression to predict carcass weight in beef cattle in advance of the slaughter," *Comput. Electron. Agricult.*, vol. 91, no. 2, pp. 116–120, 2013.
[40] N. Liu, X. Cui, D. M. Bryant, and G. H. Glover, "Inferring deep-brain activity from cortical activity using functional near-infrared spectroscopy," *Biomed. Opt. Exp.*, vol. 6, no. 3, pp. 1074–1089, 2015.
[41] R. Eberhart and J. Kennedy, "A new optimizer using particle swarm theory," in *Proc. IEEE Int. Symp. MICRO Mach. Hum. Sci.*, Nagoya, Japan, Oct. 1995, pp. 39–43.
[42] D. H. Tungadio, J. A. Jordaan, and M. W. Siti, "Power system state estimation solution using modified models of PSO algorithm: Comparative study," *Measurement*, vol. 92, pp. 508–523, Oct. 2016.
[43] K. E. Parsopoulos and M. N. Vrahatis, "Particle swarm optimization method in multiobjective problems," *ACM Symp. Appl. Comput.*, vol. 76, no. 1, pp. 603–607, 2002.
[44] L. Liu, W. Liu, and D. A. Cartes, "Particle swarm optimization-based parameter identification applied to permanent magnet synchronous motors," *Eng. Appl. Artif. Intell.*, vol. 21, no. 7, pp. 1092–1100, 2008.
[45] B. Lei *et al.*, "Optimal and secure audio watermarking scheme based on self-adaptive particle swarm optimization and quaternion wavelet transform," *Signal Process.*, vol. 113, pp. 80–94, Aug. 2015.
[46] J. Zhang and P. Xia, "An improved PSO algorithm for parameter identification of nonlinear dynamic hysteretic models," *J. Sound Vibrat.*, vol. 389, pp. 153–167, Feb. 2016.
[47] J. Sun and X. Liu, "A novel APSO-aided maximum likelihood identification method for Hammerstein systems," *Nonlinear Dyn.*, vol. 73, nos. 1–2, pp. 449–462, 2013.
[48] M. Taherkhani and R. Safabakhsh, "A novel stability-based adaptive inertia weight for particle swarm optimization," *Appl. Soft. Comput.*, vol. 38, pp. 281–295, Jan. 2016.
[49] Y. Shi and R. Eberhart, "A modified particle swarm optimizer," in *Proc. IEEE Int. Conf. Evol. Comput.*, Anchorage, AK, USA, May 1998, pp. 69–73.
[50] A. J. Smola and B. Schölkopf, "A tutorial on support vector regression," *Statist. Comput.*, vol. 14, no. 3, pp. 199–222, Aug. 2004.
[51] V. N. Vapnik, "An overview of statistical learning theory," *IEEE Trans. Neural Netw.*, vol. 10, no. 5, pp. 988–999, Sep. 1999.
[52] C. C. Chang and C. J. Lin, "LIBSVM: A library for support vector machines," *ACM Trans. Intell. Syst. Technol.*, vol. 2, no. 3, pp. 1–27, 2011.

**AINI DAI** received the M.S. degree in electric power system and automation from Qingdao University, Qingdao, China, in 2005. She is currently pursuing the Ph.D. degree in control science and engineering with the School of Automation, Beijing University of Posts and Telecommunications, Beijing, China. From 2005 to 2018, she was a Lecturer with the Science and Information College, Qingdao Agriculture University, Qingdao. Her research interests include the development of grain drying control, control systems, intelligent control, and industrial control.

**XIAOGUANG ZHOU** received the M.S. degree from the Department of Precision Instrument, Tsinghua University, in 1984, and the Ph.D. degree in engineering from the Tokyo University of Agriculture and Technology, Japan. He was a Visitor Professor with the Tokyo University of Agriculture and Technology from 2001 to 2002, and a JSPS Researcher with Tokyo University from 2013 to 2014. He is currently a Professor, and a Doctoral Supervisor with the School of Automation, Beijing University of Posts and Telecommunications. He also serves as the Director of the Engineering Research Center of Information Networks, Ministry of Education. He is the author of over 10 books, over 100 articles, and over 16 inventions. His research interests include control theory and its application in engineering, Internet of Things and automated logistics system, and mechatronics technology. He is a permanent member of the Chinese Association of Automation/Manufacturing Technology Committee and the China Institute of Communications/Equipment manufacturing technical Committee.

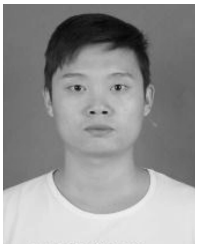

**HAO DANG** received the M.S. degree in pattern recognition and intelligent system from the Henan University of Technology, Zhengzhou, China, in 2016. He is currently pursuing the Ph.D. degree in control science and engineering with the School of Automation, Beijing University of Posts and Telecommunications, Beijing, China. His research interests include the pattern recognition, intelligent systems, and so on.

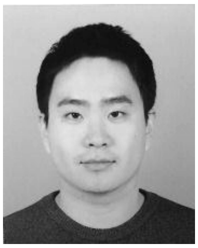

**MUYI SUN** received the B.S. degree in automation from the Beijing University of Posts and Telecommunications, Beijing, China, in 2015, where he is currently pursuing the Ph.D. degree in control science and engineering with the School of Automation. His research interests include the pattern recognition, intelligent systems, and so on.

**ZIDAN WU** received the degree from the Zhengzhou Grain College, Zhengzhou, China, in 1982. He was a Researcher and the Head of the National Engineering Laboratory for Grain Storage and Transportation from 2009 to 2011. He is currently the Chief Expert of grain storage and logistics in the Chinese Cereals and Oil Association. He has been an Adjunct Professor and a Doctoral Supervisor with the Beijing University of Posts and Telecommunications since 2009. He is the author of five books and 14 inventions. His research interests include grain storage and logistics technology, logistics information technology, and so on. He received the first prize of the National Science and Technology Progress Award in 2010.